View metadata, citation and similar papers at core.ac.uk

brought to you by CORE

provided by Repository of the University of Namur

Institutional Repository - Research Portal
Dépôt Institutionnel - Portail de la Recherche

researchportal.unamur.be

RESEARCH OUTPUTS / RÉSULTATS DE RECHERCHE

# Decoration of tricarboxylic and monocarboxylic aryl diazonium functionalized multi-wall carbon nanotubes with iron nanoparticles

Bhakta, Arvind Kumar; Detriche, Simon; Martis, Praveen; Mascarenhas, Ronald J.; Delhalle, Joseph; Mekhalif, Zineb

*Published in:*
Journal of Materials Science

*DOI:*
10.1007/s10853-017-1100-z

*Publication date:*
2017

*Document Version*
Publisher's PDF, also known as Version of record

Link to publication

*Citation for pulished version (HARVARD):*
Bhakta, AK, Detriche, S, Martis, P, Mascarenhas, RJ, Delhalle, J & Mekhalif, Z 2017, 'Decoration of tricarboxylic and monocarboxylic aryl diazonium functionalized multi-wall carbon nanotubes with iron nanoparticles' Journal of Materials Science, vol. 52, no. 16, pp. 9648-9660. https://doi.org/10.1007/s10853-017-1100-z

**General rights**
Copyright and moral rights for the publications made accessible in the public portal are retained by the authors and/or other copyright owners and it is a condition of accessing publications that users recognise and abide by the legal requirements associated with these rights.

- Users may download and print one copy of any publication from the public portal for the purpose of private study or research.
- You may not further distribute the material or use it for any profit-making activity or commercial gain
- You may freely distribute the URL identifying the publication in the public portal ?

**Take down policy**
If you believe that this document breaches copyright please contact us providing details, and we will remove access to the work immediately and investigate your claim.

Download date: 21. May. 2019

*J Mater Sci*

**Energy materials**

# Decoration of tricarboxylic and monocarboxylic aryl diazonium functionalized multi-wall carbon nanotubes with iron nanoparticles

Arvind K. Bhakta[1], S. Detriche[1], P. Martis[2], R. J. Mascarenhas[3], J. Delhalle[1], and Z. Mekhalif[1,*]

[1] *Laboratory of Chemistry and Electrochemistry of Surfaces, University of Namur, 61 Rue de Bruxelles, 5000 Namur, Belgium*
[2] *Loyola Centre for Research and Innovation, St. Aloysius College, Light House Hill Road, Mangalore, Karnataka 575003, India*
[3] *Electrochemistry Research Group, Department of Chemistry, St. Joseph's College, Lalbagh Road, Bangalore, Karnataka 560027, India*

**Received:** 3 March 2017
**Accepted:** 13 April 2017

© Springer Science+Business Media New York 2017

## ABSTRACT

A simple, reliable, reproducible, and efficient method to decorate multi-wall carbon nanotubes (MWCNTs) with iron nanoparticles is presented. Purified MWCNTs are first functionalized with mono- and tricarboxylic aryl diazonium salts generated in situ, then iron nanoparticles are formed using iron (II) acetate. Different characterization techniques (XPS, TEM, PXRD, and FESEM) are used to assess the properties of the resulting materials. Homogeneous distribution of iron nanoparticles on MWCNTs is evidenced with a Gaussian mean diameter of $\sim 2.7 \pm 0.2$ and $\sim 3.8 \pm 0.3$ nm for monocarboxylic and tricarboxylic functionalizations, respectively. Obtaining such a small size homogeneously distributed iron nanoparticles on MWCNTs is the main achievement of this work. Furthermore, nanoparticles based on tricarboxylic aryl diazonium functions, used for the first time to functionalize CNTs, are more crystalline and essentially in the metallic state. This opens interesting perspectives for nanotechnology. The present methodology is also applicable to large-scale preparation.

## Introduction

Carbon nanotubes (CNTs) have received great attention due to their extraordinary tensile strength, high chemical stability, large surface area, excellent electrical and high thermal conductivities [1]. These CNTs properties have potential applications in the field of hydrogen storage [2], solar and fuel cells, lithium ion batteries, supercapacitors [3], nanotweezers [4], quantum wires [5], field emission sources [6], electronic devices [7], chemical and biosensors [8, 9], to cite a few. The efficient photo-absorption and photo-thermal conversion properties of CNTs in the near-infrared (IR) region make them prone to be used as near-IR functional materials [10]. CNTs absorb near-IR radiation, quickly transferring electronic excitations into molecular vibration energies resulting in heat [11]. Accordingly, CNTs have

Address correspondence to E-mail: zineb.mekhalif@unamur.be

DOI 10.1007/s10853-017-1100-z

Published online: 26 April 2017

been suggested as the ideal metal catalyst support for sensing and electrocatalytic applications [12–16].

As-prepared CNTs contain impurities like by-product carbonaceous species, metallic catalyst. Furthermore, CNTs are insoluble in most solvents because of the strong van der Waals interactions that firmly hold them together in bundles. This affects the unique properties of CNTs [17]. Different methods of CNTs functionalization to enhance their solubility and dispersion in various solvents have been reported. In particular, treatments with acids [18] and oxidants [19] increase their solubility in water. Reaction with (R-)-oxycarbonyl nitrenes [20] leads to the functionalization of CNTs with different groups such as dendrimers, aromatic groups, crown ethers, alkyl chains, and oligoethylene glycol units which allows significant increase in the solubility in organic solvents like dimethyl sulfoxide (DMSO), 1,2-dichlorobenzene (ODCB) and 1,1,2,2-tetrachloroethane (TCE). Prato reaction [21] applied to CNTs enhances their solubility in $CH_2Cl_2$, $CHCl_3$, ethanol, methanol, acetone, and also water. Derivatization [22] with thionychloride and octadecylamine leads to an increase of CNTs solubility in common organic solvents. Electrochemical methods were also employed to functionalize CNTs [23, 24]. Diazonium chemistry plays a very important role in the nano-research areas [25, 26].

Nanoparticles possess unique optical, chemical, and magnetic properties resulting from their small size. Magnetic nanoparticles have applications in electrical components (e.g., transformers) [27], diagnosis and treatment of diseases [28], transducer and sensor applications [29]. These properties are most effective with very small particle size (<10–20 nm). In many cases, these effects decrease when particles size increases and essentially disappear for sizes beyond 40–50 nm. Iron nanoparticles are also used as catalysts [30–32]. Iron (zerovalent) nanoparticles exhibit high reactivity towards the transformation of pollutants and hence are widely used for the treatment of hazardous waste, remediation of soil and groundwater [33–37]. Iron nanoparticles play an important role in biomedical applications [38] where they have also been considered as potential magnetic carriers [39]. CNTs are highly hydrophobic in nature and chemically stable. Due to these properties, CNTs decoration with magnetic NPs of several to tens of nanometres of elements or compounds [40–49] are usually achieved by wet chemistry. Other methods use thermal decomposition [50, 51] and electrodeposition [52].

Methods for the decoration of iron nanoparticles on CNTs have been reported but have still certain limitations to overcome like control of particle size and distribution, chemical state of the particles and their purity, process simplicity [53–57]. In this work, we aim to control the size, concentration, nature, and distribution of iron nanoparticles on MWCNTs. This is achieved using IR irradiation [58–63] to functionalize purified multi-wall carbon nanotubes (p-MWCNTs) with mono- (p-MWCNTs-D1) and tricarboxylic aryl diazonium (p-MWCNTs-D3) and impregnate them with iron nanoparticles.

## Materials and methods

### Chemicals

All the chemicals are of analytical grade or higher purity and used as such. NaOH (>98%) and iron (II) acetate (95%) are purchased from Acros Organics. Sodium nitrite (99.2%), 5-amino-1,2,3-benzenetricarboxylic acid (97%), 4-aminobenzoic acid (99%), perchloric acid (70%), pentane (99%), and acetone (>99%) are obtained from Fisher Scientific UK, ABCR GmbH &CO.KG, Aldrich, Merck Eurolab nv/sa, Lab-Scan Analytical Sciences and Chem-Lab, respectively. All aqueous solutions are made using ultra-pure water. The thin MWCNTs (NC 7000) (>95%) received from Nanocyl SA (Belgium) have length of several (0.1–10) μm with an average diameter of 10 nm.

### Apparatus

Irradiation of the samples during the impregnation step is carried out using a Petra IR 11 IR lamp (capacity: 150 W, 50/60 Hz, voltage: 230 V). XPS spectra are recorded on a Thermo Scientific K-Alpha spectrometer using monochromatized Al Kα radiation (1486.6 eV), and the photoelectrons collected at 0° with respect to the surface normal are analysed using a hemispherical analyser. The major peak of core-level spectra is calibrated with respect to C1 s level fixed at 284.6 eV. The spot size of the X-ray source on the sample is 200 μm, and the analyser is operated with a pass energy of 200 and 50 eV for survey and high-resolution core levels spectra, respectively. XPS samples were prepared by making use of aluminium

plate. Scotch tape is cut into small square pieces and pasted onto the aluminium plate. The sticky end of the scotch tape is exposed by removing the paper from it. The sample is kept on the top of it, and it is pressed using spatula to fix the sample and then excess sample is removed using suction. Transmission electron microscopy (TEM) analyses are carried out using Tecnai 10 Philips microscope. Samples for TEM analysis are prepared by dispersing the material in ethanol and depositing a drop of suspension on a carbon-coated copper grid. TEM was operated with 80 kV accelerating voltage, 5 μA emission current and spot size 3. Powder X-Ray diffraction (PXRD) is performed using PAN analytical XPert PRO Bragg–Brentano diffractometer with tube current of 30 mA and an operating voltage of 45 kV with Cu Kα ($\lambda = 1.5418$ Å) in the $2\theta$ range of 10°–90°. Field emission scanning electron microscopy (FESEM) studies are carried out using a JEOL JSM-7500F microscope operating at 15 kV at a working distance of 4.2 mm.

## Purification of crude MWCNTs

The process of purification is as follows: 1 g of crude MWCNTs is mixed with 100 ml of 12 M NaOH [64] solution in a round-bottomed flask. The above suspension is then heated under constant agitation at 170 °C for 12 h. The mixture is cooled, filtered, and washed with water until neutral pH and ultimately washed with acetone and dried in air. The purified MWCNTs are referred to as p-MWCNTs.

## Carboxylic aryl diazonium functionalization of p-MWCNTs

In the present case, p-MWCNTs (80 mg) are mixed with 5-amino-1,2,3-benzenetricarboxylic acid (150 mg, 0.67 mmol), water (10 ml), sodium nitrite (46 mg, 0.67 mmol), and perchloric acid (69 μl, 1.14 mmol). The mixture is then IR irradiated under constant magnetic stirring for 1 h, then cooled down to room temperature, and filtered, and the residue is washed with pentane followed by acetone and finally, dried at room temperature. The tricarboxylic aryl diazonium functionalized MWCNTs thus obtained are referred to hereafter as p-MWCNTs-D3. Similarly, the monocarboxylic diazonium functionalized MWCNTs (p-MWCNTs-D1) are obtained with 4-aminobenzoic acid (91 mg, 0.66 mmol) according to the above procedure.

## Impregnation of Iron (II) acetate on p-MWCNTs-D3 and p-MWCNTs-D1

0.1739 g of iron (II) acetate (IA) is dissolved in 100 ml of water. The functionalized CNTs (p-MWCNTs-D3 or p-MWCNTs-D1) are added into the above solution. The mixture is sonicated for 5 min and then IR irradiated under constant magnetic stirring for 2 h. The mixture is cooled to room temperature and filtered, and the residue is washed with water followed by acetone and dried in air. The impregnated p-MWCNTs thus obtained are referred to hereafter as p-MWCNTs-D3/IA and p-MWCNTs-D1/IA.

## Calcination of p-MWCNTs-D3/IA and p-MWCNTs-D1/IA

The p-MWCNTs-D3/IA and p-MWCNTs-D1/IA are calcined in a tubular furnace equipped with a quartz tube maintained at 500 °C under a continuous flow of argon gas for 2 h. The obtained materials are labelled as p-MWCNTs-D3/Fe and p-MWCNTs-D1/Fe, respectively.

# Results and discussion

Carbon nanotubes are characterized (XPS, TEM, PXRD, and FESEM) and compared at each step of their modifications (purification, functionalization, impregnation and calcination).

## Materials chemical composition by XPS

Figure 1 shows the XPS general survey spectra of p-MWCNTs, p-MWCNTs-D3, p-MWCNTs-D1, p-MWCNTs-D3/IA, p-MWCNTs-D1/IA, p-MWCNTs -D3/Fe and p-MWCNTs-D1/Fe. Percentage compositions of these materials are displayed in Table 1. Absence of alumina and silica in p-MWCNTs (Fig. 1a) validates the efficiency of the purification method of MWCNTs. The peak at 285.3 eV, in all cases, is attributed to $Csp^2$—hybridized carbon in the graphitic layers of the CNTs. The presence of O1 s and N1 s (Fig. 1b, c) indicates that MWCNTs are functionalized with tricarboxylic and monocarboxylic aryl diazonium groups. Impregnation of IA on

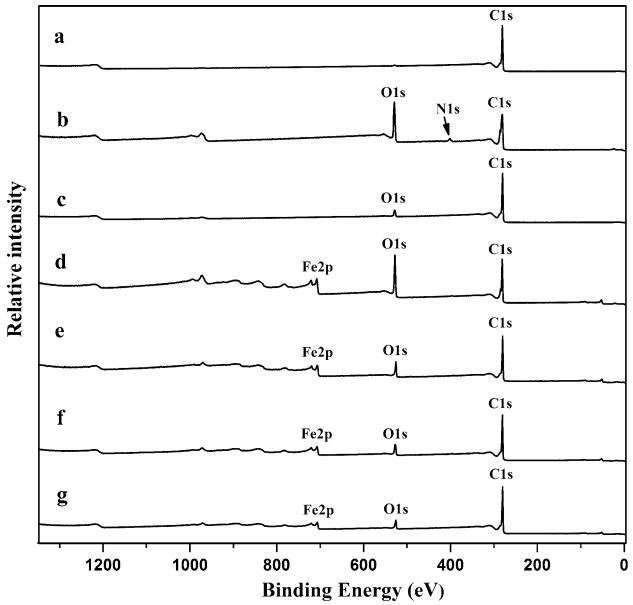


**Figure 1** XPS survey spectra of *a* p-MWCNTs, *b* p-MWCNTs-D3, *c* p-MWCNTs-D1, *d* p-MWCNTs-D3/IA, *e* p-MWCNTs-D1/IA, *f* p-MWCNTs-D3/Fe, and *g* p-MWCNTs-D1/Fe.

**Table 1** Chemical composition of different materials obtained from XPS analysis

| Material | C% | O% | N% | Fe% |
|---|---|---|---|---|
| p-MWCNTs | 98.50 | 1.50 | – | – |
| p-MWCNTs-D3 | 72.85 | 23.87 | 3.28 | – |
| p-MWCNTs-D1 | 92.87 | 6.59 | 0.54 | – |
| p-MWCNTs-D3/IA | 67.46 | 25.34 | 1.29 | 5.91 |
| p-MWCNTs-D1/IA | 83.89 | 10.17 | 1.04 | 4.89 |
| p-MWCNTs-D3/Fe | 82.94 | 11.25 | – | 5.42 |
| p-MWCNTs-D1/Fe | 89.01 | 7.33 | – | 3.63 |

carboxylic functions is confirmed by the presence of the Fe2p peak (Fig. 1d, e) which remains after heat treatment (Fig. 1f, g).

XPS C1 s core-level spectra of p-MWCNTs (97.82% C and 2.73% O), p-MWCNTs-D3 (74.20% C and 27.98% O), p-MWCNTs-D1 (96.72% C and 5.44% O), p-MWCNTs-D3/IA (86.48% C and 23.63% O), p-MWCNTs-D1/IA (97.87% C and 3.61% O), p-MWCNTs-D3/Fe(96.81% C and 4.30% O), and p-MWCNTs-D1/Fe (97.53% C and 3.32% O) are shown in Fig. 2. The C1 s region of p-MWCNTs-D3 (Fig. 2b) contains seven peaks [65, 66]. The broad and highly intense peak at 284.6 eV is ascribed to $sp^2$-hybridized graphitic carbon, and the one at 285.9 eV is due to $sp^3$-hybridized carbon resulting from structural defects on CNTs outer surface. The peak at 286.7 eV corresponds to carbon–oxygen single bonds (C–O). Carbon bounds to oxygen through double bonds (C=O) appear at 287.6 eV, while carbons bound to two oxygen atoms (–COO) appear at 289.1 eV. The shake-up peak at 290.6 eV is characteristic of the aromatic character of CNTs, while the peak at 283.9 eV results from an artefact from the spectrometer [67]. Similar peaks, especially those of the shake-up and the carboxylic groups, are present with lower intensities in the case of p-MWCNTs-D1 (Fig. 2c). This clearly evidences the presence of carboxylic acid groups in both cases but with a larger relative amount for p-MWCNTs-D3. The amount of oxygen present in these high-resolution spectra are almost in good correlation with that reported in the survey spectra of p-MWCNTs, p-MWCNTs-D3, p-MWCNTs-D1, and p-MWCNTs-D3/IA. The amount of oxygen found in high-resolution spectra of p-MWCNTs-D1/IA, p-MWCNTs-D3/Fe, and p-MWCNTs-D1/Fe are more than those reported in the survey spectra. The slight differences found in the amount of oxygen present in high resolution and survey spectra for p-MWCNTs and p-MWCNTs-D1 can be attributed to the presence of physisorbed water. The differences for p-MWCNTs-D3 may be due to physisorbed water as well as presence of CN bonds. The differences arise in the p-MWCNTs-D3/IA may be result of physisorbed water, CN bonds and presence of FeO on the surface of the CNTs. The differences arise for p-MWCNTs-D1/IA, p-MWCNTs-D3/Fe, and p-MWCNTs-D1/Fe can be assigned to the contribution of oxygen from FeO.

High-resolution XPS spectra obtained from O1 s and Fe2p are displayed in Figs. 3 and 4, respectively.

## Materials morphology by TEM and FESEM

TEM image of p-MWCNTs (Fig. S1 supplementary information) indicates that the nanotubes keep their integrity after the purification process. TEM images of p-MWCNTs-D3 (Fig. 5a) and p-MWCNTs-D1 (Fig. 5d) show that the nanotubes remain intact after the functionalization step, which is a definite advantage over acid treatments known to damage the tubes [22]. Indeed, chemical oxidation is one of the common methods to purify CNTs. This includes electrochemical oxidation, gas phase oxidation (using $O_2$, air, $H_2O$, $Cl_2$, etc.), and liquid phase oxidation (acid treatment and refluxing, etc.) [68]. The normally used oxidants for liquid phase oxidation include $HNO_3$ [69–71], $H_2O_2$ or a mixture of $H_2O_2$ and HCl

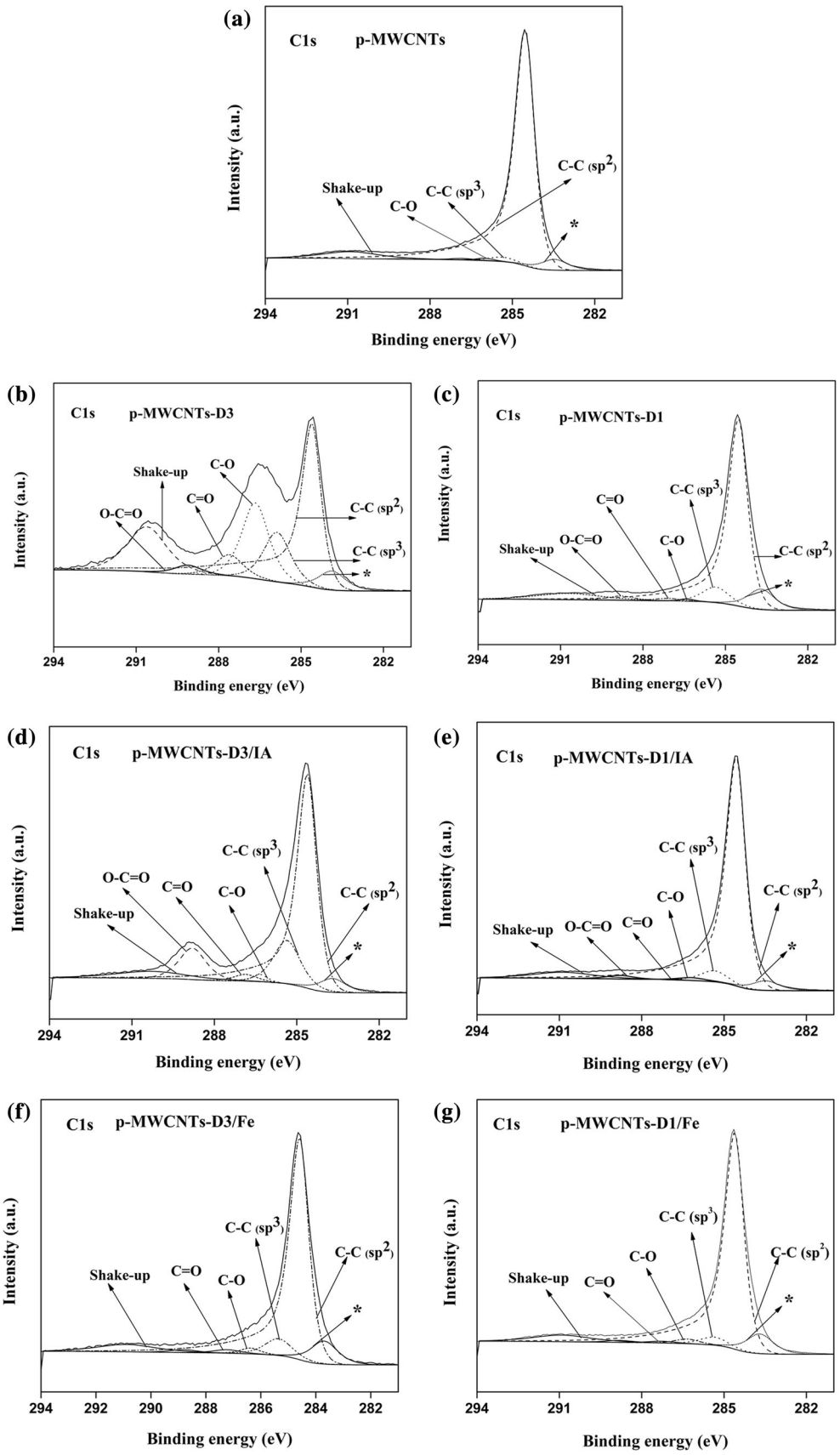


**Figure 2** Core-level XPS spectra C1 s regions of **a** p-MWCNTs, **b** p-MWCNTs-D3, **c** p-MWCNTs-D1, **d** p-MWCNTs-D3/IA, **e** p-MWCNTs-D1/IA, **f** p-MWCNTs-D3/Fe, and **g** p-MWCNTs-D1/Fe.

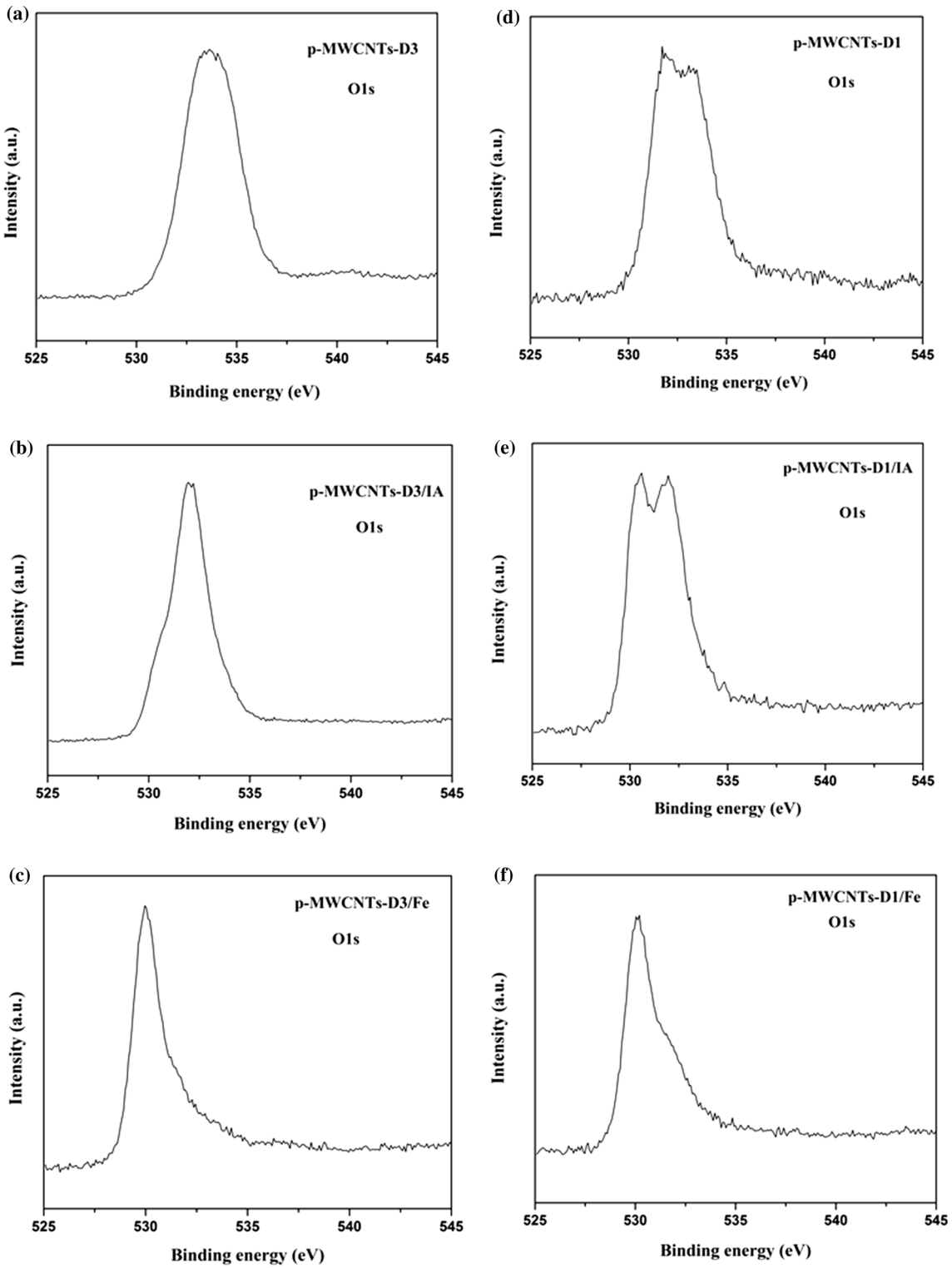


**Figure 3** High-resolution XPS spectra of core O1 s of **a** p-MWCNTs-D3, **b** p-MWCNTs-D3/IA, **c** p-MWCNTs-D3/Fe, **d** p-MWCNTs-D1, **e** p-MWCNTs-D1/IA, **f** p-MWCNTs-D1/Fe.

[72–74], $KMnO_4$ [75–77] and mixture of $H_2SO_4$ and $HNO_3$ [78]. The disadvantages of chemical oxidation methods are to form undesired reaction products on the surface of CNTs, cut CNTs, often open the extremities of CNTs, damage surface structure and incorporate oxygenated functional groups (–CO,

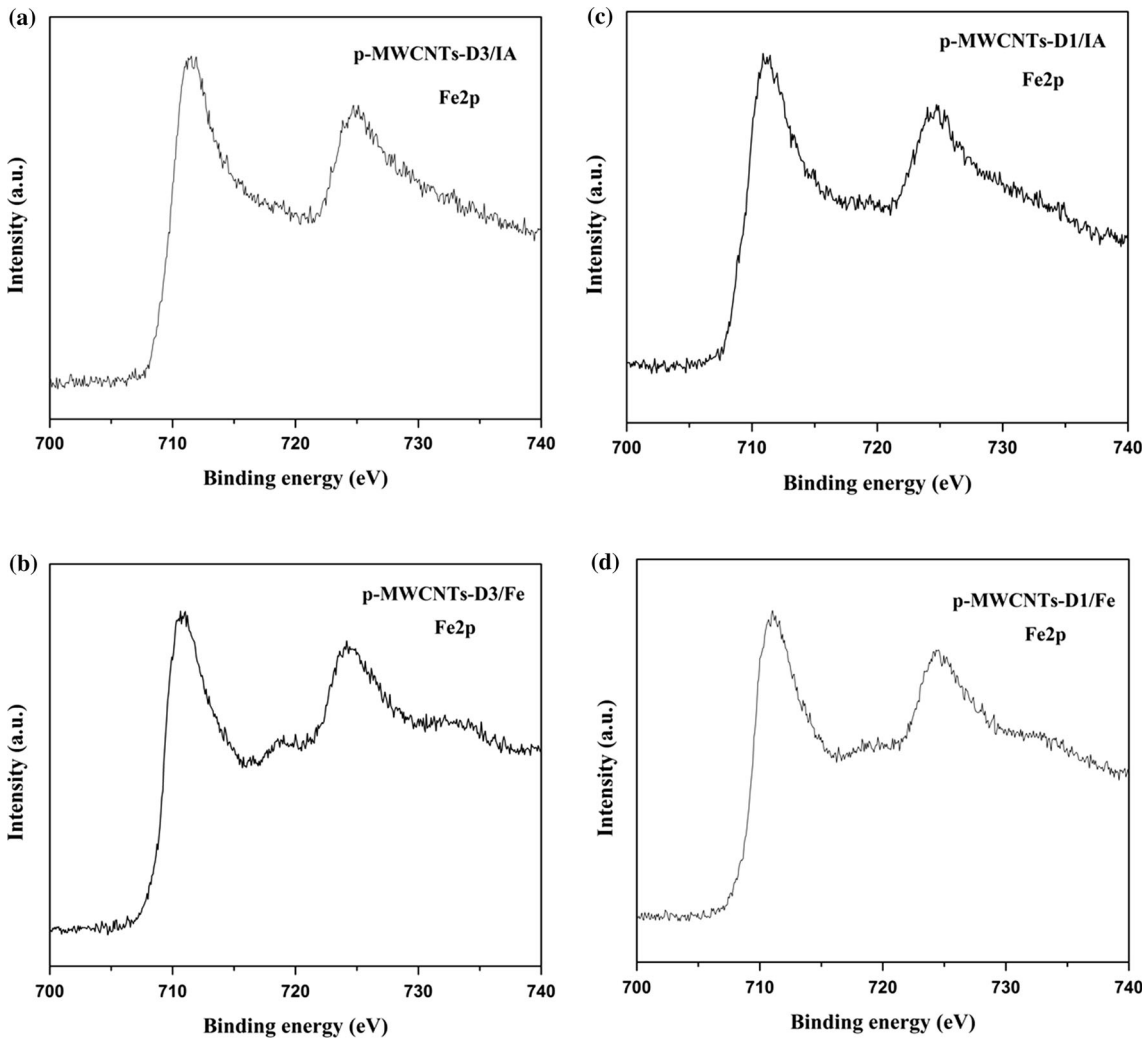


**Figure 4** High-resolution XPS spectra of core Fe2p of **a** p-MWCNTs-D3/IA, **b** p-MWCNTs-D3/Fe, **c** p-MWCNTs-D1/IA, **d** p-MWCNTs-D1/Fe.

–OH, –COOH, …) on the CNTs surface. The above results also validate the effectiveness of the carboxylic aryl diazonium functionalization using IR irradiation. Figure 5b and e shows the presence of an amorphous iron layer for both p-MWCNTs-D3/IA and p-MWCNTs-D1/IA with a larger density in the case of p-MWCNTs-D3/IA. This uniform iron layer confirms that not only the particles distribution but also the carboxylic aryl diazonium functionalization on p-MWCNTs is uniform. After calcination, iron nanoparticles are formed. Their diameter on the p-MWCNTs-D3/Fe (Fig. 5c) surface measured from TEM is in the range of 1–8 nm, with a Gaussian mean diameter of $\sim 3.8 \pm 0.3$ nm (Fig. 6a). In the case of p-MWCNTs-D1/Fe (Fig. 5f), the range is of 1–5 nm, with a Gaussian mean diameter of $\sim 2.7 \pm 0.2$ nm (Fig. 6b). The fact that these iron nanoparticles are still present on the CNTs surface after the various treatments indicates that they are strongly attached. There are other different methods in the literature for decoration of CNTs with iron or iron oxide nanoparticles, but these methodologies result in clusters of nanoparticles (due to aggregation) [79, 80], comparatively very large particle size [46, 81] and non-homogeneous decoration [42, 82–85]. The present approach is free from all of these complications. Thus, obtaining a small size homogeneously distributed iron nanoparticles on MWCNTs is the main achievement of this work.

FESEM studies were carried out to further assess the surface morphology of all samples. The images of p-MWCNTs (Fig. S2), p-MWCNTs-D3 (Fig. S3 a), and

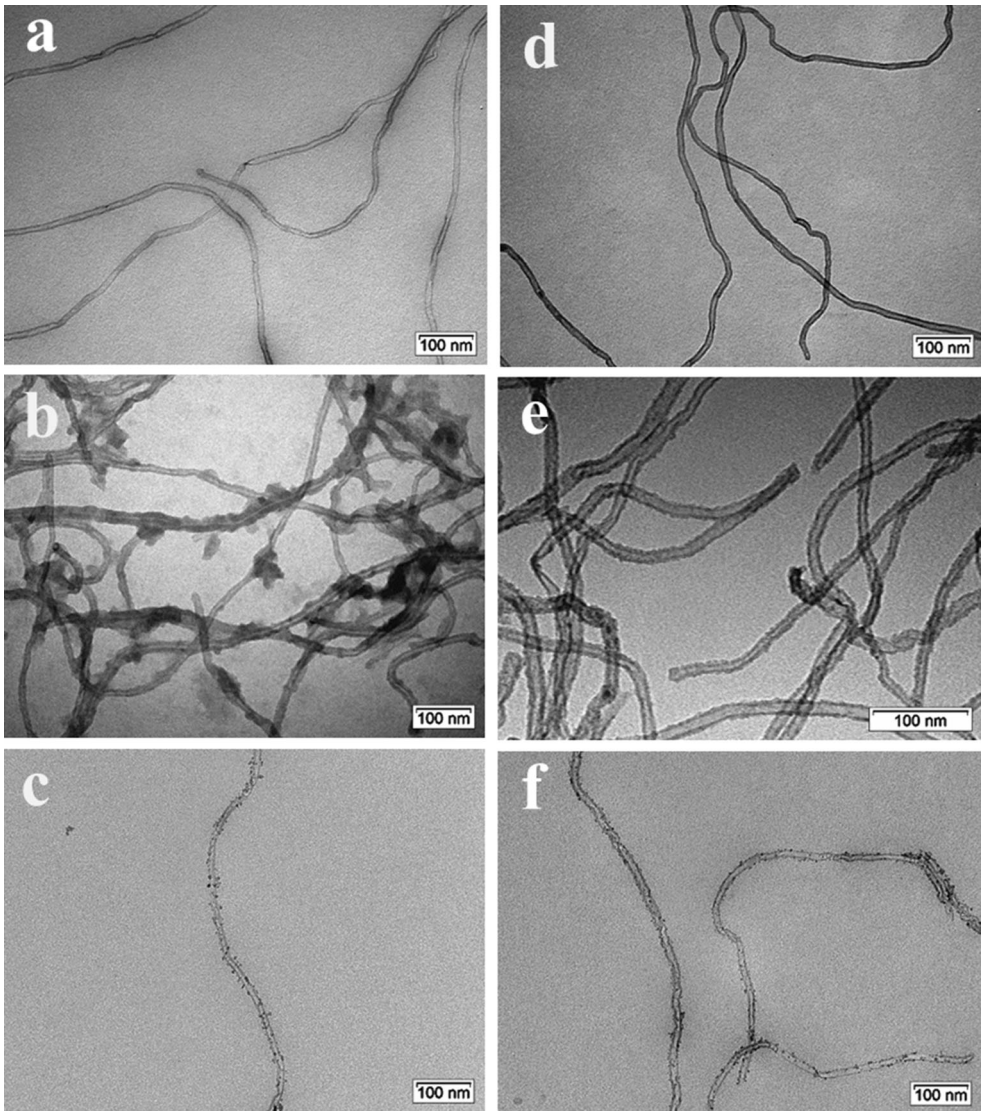


**Figure 5** TEM images of **a** p-MWCNTs-D3, **b** p-MWCNTs-D3/IA, **c** p-MWCNTs-D3/Fe, **d** p-MWCNTs-D1, **e** p-MWCNTs-D1/IA, and **f** p-MWCNTs-D1/Fe.

p-MWCNTs-D1 (Fig. S3 d) show smooth surface as expected since there is no decoration of particles. The nanoparticles are visible on decorated MWCNTs (Fig. S3c and Fig. S3f).

## Characterization of materials by PXRD

The PXRD patterns of decorated MWCNTs before and after calcination are illustrated in Fig. 7.

The diffraction peak at $2\theta = 25.8°$, due to (002) planes of graphitic carbon in MWCNTs structure is seen in all cases. Figure 7c, related to p-MWCNTs-D3/Fe, shows different peaks. The iron crystal is body centred cubic (bcc) with diffraction peaks at $2\theta = 44.7°$ (110), 63.01° (200), and 82.37° (211) [86]. The very sharp peak at $2\theta = 44.7°$ indicates the crystalline nature of iron nanoparticles, while the one at $2\theta = 35.7°$ is characteristic of zerovalent iron (α-Fe) and iron oxide (FeO) crystalline phases [87].

No sharp iron phases reflection is observed in the case of samples p-MWCNTs-D3/IA (Fig. 7a) and p-MWCNTs-D1/IA (Fig. 7b) since the impregnated particles of the composites are usually amorphous before calcination. Even after calcination, there is no

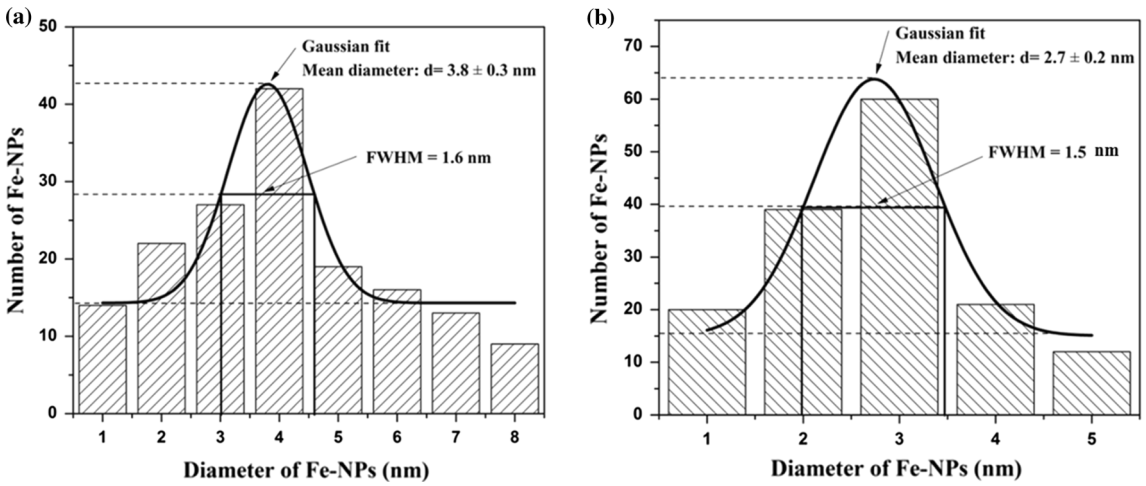


**Figure 6** Diameter distributions of the Fe-NPs of **a** p-MWCNTs-D3/Fe, and **b** p-MWCNTs-D1/Fe.

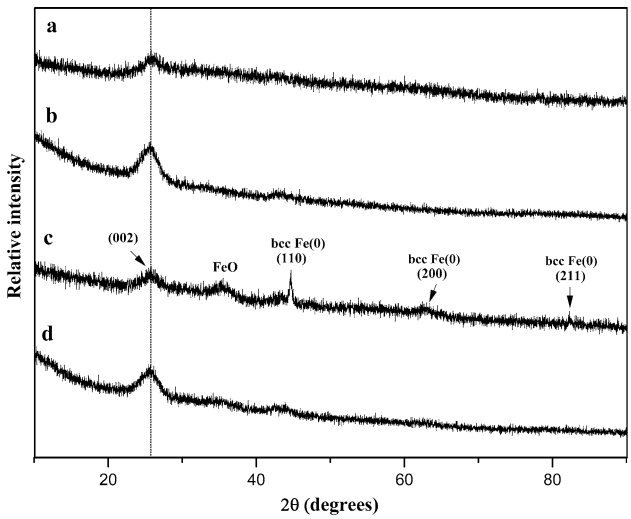


**Figure 7** PXRD patterns of *a* p-MWCNTs-D3/IA, *b* p-MWCNTs-D1/IA, *c* p-MWCNTs-D3/Fe, and *d* p-MWCNTs-D1/Fe.

sharp reflection observed for p-MWCNTs-D1/Fe (Fig. 7d), indicating that resulting iron nanoparticles are less crystalline in nature.

## Conclusions

A simple, reliable, reproducible, and efficient method is applied to impregnate iron-containing nanoparticles on p-MWCNTs-D3 and p-MWCNTs-D1 using iron (II) acetate as iron precursor by IR irradiation. Iron nanoparticles are uniformly decorated on p-MWCNTs-D3 and p-MWCNTs-D1, and their morphology and structure are investigated by various techniques.

The calcination of the iron-treated MWCNTs leads to two size ranges of iron nanoparticles, obtained through the use of two (mono- and tricarboxylic diazonium salts) different functionalizations of MWCNTs. Iron nanoparticles size range varies from 1 nm to 5 nm with a Gaussian mean diameter of $\sim 2.7 \pm 0.2$ nm and, from 1 to 8 nm with a Gaussian mean diameter of $\sim 3.8 \pm 0.3$ nm. Loading of Fe on the surface of MWCNTs is more important in the case of tricarboxylic functions than the monocarboxylic ones. This is mainly due the effect of 3 COOH groups. Furthermore, nanoparticles based on tricarboxylic aryl diazonium functions, used for the first time to functionalize CNTs, are more crystalline and essentially in the metallic state. This clearly proves the superiority of tricarboxylic aryl diazonium functions over monocarboxylic aryl diazonium ones. The present methodology is also applicable to large-scale preparation. The as-prepared iron nanoparticles decorated MWCNTs are expected to have synergistic effects and hence would be of use in many potential applications such as electronic devices, energy storage and conversion system, chemical and biosensor.

## Acknowledgements

Arvind K. Bhakta thanks the University of Namur for a CERUNA doctoral fellowship.

## Compliance with ethical standards

**Conflict of interest** The authors declare that there is no conflict of interest.

**Electronic supplementary material:** The online version of this article (doi:10.1007/s10853-017-1100-z) contains supplementary material, which is available to authorized users.

## References


[1] Ajayan PM (1999) Nanotubes from carbon. Chem Rev 99:1787–1799

[2] Chen P, Wu X, Lin J, Tan KL (1999) High $H_2$ uptake by alkali-doped carbon nanotubes under ambient pressure and moderate temperatures. Science 285:91–93

[3] Yang Z, Ren J, Zhang Z, Chen X, Guan G, Qiu L, Zhang Y, Peng H (2015) Recent advancement of nanostructured carbon for energy applications. Chem Rev 115:5159–5223

[4] Kim P, Lieber CM (1999) nanotube nanotweezers. Science 286:2148–2150

[5] Tans SJ, Devoret MH, Dai H, Thess A, Smalley RE, Geerligs LJ, Dekker C (1997) Individual single-wall carbon nanotubes as quantum wires. Nature 386:474–477

[6] Milne WI, Teo KBK, Amaratunga GAJ, Legagneux P, Gangloff L, Schnell J-P, Semet V, Thien Binh V, Groening O (2004) Carbon nanotubes as field emission sources. J Mater Chem 14:933–943

[7] Li J, Zhang Q, Yang D, Tian J (2004) Fabrication of carbon nanotube field effect transistors by AC dielectrophoresis method. Carbon 42:2263–2267

[8] Kong J, Franklin NR, Zhou C, Chapline MG, Peng S, Cho K, Dai H (2000) Nanotube molecular wires as chemical sensors. Science 287:622–625

[9] Wohlstadter JN, Wilbur JL, Sigal GB, Biebuyck HA, Billadeau MA, Dong L, Fischer AB, Gudibande SR, Jameison SH, Kenten JH, Leginus J, Leland JK, Massey RJ, Wohlstadter SJ (2003) Carbon nanotube based biosensor. Adv Mater 15:1184–1187

[10] Narimatsu K, Niidome Y, Nakashima N (2006) Pulsed-laser induced flocculation of carbon nanotubes solubilized by an anthracene-carrying polymer. Chem Phys Lett 429:488–491

[11] Miyako E, Nagata H, Hirano K, Hirotsu T (2008) Carbon nanotube–polymer composite for light-driven microthermal control. Angew Chem Int Ed 47:3610–3613

[12] Li S, Ma J, Huo H, Jin J, Ma J, Yang H (2016) Ionic liquids-noncovalently functionalized multi-walled carbon nanotubes decorated with palladium nanoparticles: a promising electrocatalyst for ethanol electrooxidation. Int J Hydrogen Energy 41:12358–12368

[13] Li W, Liang C, Zhou W, Qiu J, Zhou Z, Sun G, Xin Q (2003) Preparation and characterization of multiwalled carbon nanotube-supported platinum for cathode catalysts of direct methanol fuel cells. J Phys Chem B 107:6292–6299

[14] Bathinapatla A, Kanchi S, Singh P, Sabela MI, Bisetty K (2015) Fabrication of copper nanoparticles decorated multiwalled carbon nanotubes as a high performance electrochemical sensor for the detection of neotame. Biosens Bioelectron 67:200–207

[15] Zhang X, Wang G, Zhang W, Wei Y, Fang B (2009) Fixure-reduce method for the synthesis of Cu2O/MWCNTs nanocomposites and its application as enzyme-free glucose sensor. Biosens Bioelectron 24:3395–3398

[16] Chen K-J, Pillai KC, Rick J, Pan C-J, Wang S-H, Liu C-C, Hwang B-J (2012) Bimetallic PtM (M = Pd, Ir) nanoparticle decorated multi-walled carbon nanotube enzyme-free, mediator-less amperometric sensor for $H_2O_2$. Biosens Bioelectron 33:120–127

[17] Karousis N, Tagmatarchis N (2010) Current progress on the chemical modification of carbon nanotubes. Chem Rev 110:5366–5397

[18] Rahmam S, Mohamed NM, Sufian S (2014) Effect of acid treatment on the multiwalled carbon nanotubes. Mater Res Innov 18:196–199

[19] Morales-Lara F, Perez-Mendoza MJ, Altmajer-Vaz D, Garcia-Roman M, Melguizo M, Lopez-Garzon FJ, Domingo-Garcia M (2013) Functionalization of multiwall carbon nanotubes by ozone at basic pH. Comparison with oxygen plasma and ozone in gas phase. J Phys Chem C 117:11647–11655

[20] Holzinger M, Abraham J, Whelan P, Graupner R, Ley L, Hennrich F, Kappes M, Hirsch A (2003) Functionalization of single-walled carbon nanotubes with (R-)oxycarbonyl nitrenes. J Am Chem Soc 125:8566–8580

[21] Georgakilas V, Kordatos K, Prato M, Guldi DM, Holzinger M, Hirsch A (2002) Organic functionalization of carbon nanotubes. J Am Chem Soc 124:760–761

[22] Chen J, Hamon MA, Hu H, Chen Y, Rao AM, Eklund PC, Haddon RC (1998) Solution properties of single-walled carbon nanotubes. Science 282:95–98

[23] Wang Y, Malhotra SV, Owens FJ, Iqbal Z (2005) Electrochemical nitration of single-wall carbon nanotubes. Chem Phys Lett 407:68–72

[24] Burghard M, Maroto A, Balasubramanian K, Assmus T, Forment-Aliaga A, Lee EJH, Weitz RT, Scolari M, Nan F, Mews A, Kern K (2007) Electrochemically modified single-

walled carbon nanotubes. Phys Status Solidi (b) 244:4021–4025

[25] Matrab T, Chancolon J, L'hermite MM, Rouzaud J-N, Deniau G, Boudou J-P, Chehimi MM, Delamar M (2006) Atom transfer radical polymerization (ATRP) initiated by aryl diazonium salts: a new route for surface modification of multiwalled carbon nanotubes by tethered polymer chains. Colloids Surf A Physicochem Eng Asp 287:217–221

[26] Mekki A, Ait-Touchente Z, Samanta S, Singh A, Mahmoud R, Chehimi MM, Aswal DK (2016) Polyaniline-wrapped ZnO nanorod composite films on diazonium-modified flexible plastic substrates. Macromol Chem Phys 217:1136–1148

[27] Morais PC, Silva AS, Leite ES, Garg VK, Oliveira AC, Viali WR, Sartoratto PPC (2010) Tailoring magnetic nanoparticle for transformers application. J Nanosci Nanotechnol 10:1–4

[28] Su X, Zhan X, Tang F, Yao J, Wu J (2011) Magnetic nanoparticles in brain disease diagnosis and targeting drug delivery. Curr Nanosci 7:37–46

[29] Rocha-Santos TAP (2014) Sensors and biosensors based on magnetic nanoparticles, TrAC. Trends Anal Chem 62:28–36

[30] Huber DL (2005) Synthesis, properties, and applications of iron nanoparticles. Small 1:482–501

[31] Suslick KS, Hyeon T, Fang M (1996) Nanostructured materials generated by high-intensity ultrasound: sonochemical synthesis and catalytic studies. Chem Mater 8:2172–2179

[32] Gai C, Zhang F, Lang Q, Liu T, Peng N, Liu Z (2017) Facile one-pot synthesis of iron nanoparticles immobilized into the porous hydrochar for catalytic decomposition of phenol. Appl Catal B Environ 204:566–576

[33] Yanez H JE, Wang Z, Lege S, Obst M, Roehler S, Burkhardt CJ, Zwiener C (2017) Application and characterization of electroactive membranes based on carbon nanotubes and zerovalent iron nanoparticles. Water Res 108:78–85

[34] Ravikumar KVG, Dubey S, Pulimi M, Chandrasekaran N, Mukherjee A (2016) Scale-up synthesis of zero-valent iron nanoparticles and their applications for synergistic degradation of pollutants with sodium borohydride. J Mol Liq 224:589–598

[35] Zhao X, Liu W, Cai Z, Han B, Qian T, Zhao D (2016) An overview of preparation and applications of stabilized zero-valent iron nanoparticles for soil and groundwater remediation. Water Res 100:245–266

[36] Joo SH, Feitz AJ, Waite TD (2004) Oxidative degradation of the carbothioate herbicide, molinate, using nanoscale zero-valent iron. Environ Sci Technol 38:2242–2247

[37] Ponder SM, Darab JG, Mallouk TE (2000) Remediation of Cr(VI) and Pb(II) aqueous solutions using supported, nanoscale zero-valent iron. Environ Sci Technol 34:2564–2569

[38] Chen M, Yamamuro S, Farrell D, Majeticha SA (2003) Gold-coated iron nanoparticles for biomedical applications. J Appl Phys 93:7551–7553

[39] Carpenter EE (2001) Iron nanoparticles as potential magnetic carriers. J Magn Magn Mater 225:17–20

[40] Correa-Duarte MA, Grzelczak M, Salgueirino-Maceira V, Giersig M, Liz-Marzan LM, Farle M, Sierazdki K, Diaz R (2005) Alignment of carbon nanotubes under low magnetic fields through attachment of magnetic nanoparticles. J Phys Chem B 109:19060–19063

[41] Wu H-Q, Yuan P-S, Xu H-Y, Xu D-M, Geng B-Y, Wei X-W (2006) Controllable synthesis and magnetic properties of Fe–Co alloy nanoparticles attached on carbon nanotubes. J Mater Sci 41:6889–6894. doi:10.1007/s10853-006-0935-5

[42] Georgakilas V, Tzitzios V, Gournis D, Petridis D (2005) Attachment of magnetic nanoparticles on carbon nanotubes and their soluble derivatives. Chem Mater 17:1613–1617

[43] Jiang L, Gao L (2003) Carbon nanotubes-magnetite nanocomposites from solvothermal processes: formation, characterization, and enhanced electrical properties. Chem Mater 15:2848–2853

[44] Unger E, Duesberg GS, Liebau M, Graham AP, Seidel R, Kruepel F, Hoenlein W (2003) Decoration of multi-walled carbon nanotubes with noble- and transition-metal clusters and formation of CNT–CNT networks. Appl Phys A 77:735–738

[45] Stoffelbach F, Aqil A, Jerome C, Jerome R, Detrembleur C (2005) An easy and economically viable route for the decoration of carbon nanotubes by magnetite nanoparticles, and their orientation in a magnetic field. Chem Commun 36:4532–4533

[46] Huiqun C, Meifang Z, Yaogang L (2006) Decoration of carbon nanotubes with iron oxide. J Solid State Chem 179:1208–1213

[47] Wu H-Q, Cao Y-J, Yuan P-S, Xu H-Y, Wei X-W (2005) Controlled synthesis, structure and magnetic properties of Fe1-xNix alloy nanoparticles attached on carbon nanotubes. Chem Phys Lett 406:148–153

[48] Jang J, Yoon H (2003) Fabrication of magnetic carbon nanotubes using a metal-impregnated polymer precursor. Adv Mater 15:2088–2091

[49] Cheng J, Zhang X, Ye Y (2006) Synthesis of nickel nanoparticles and carbon encapsulated nickel nanoparticles supported on carbon nanotubes. J Solid State Chem 179:91–95

[50] Liu Q, Ren W, Chen Z-G, Liu B, Yu B, Li F, Cong H, Cheng H-M (2008) Direct synthesis of carbon nanotubes decorated

with size controllable Fe nanoparticles encapsulated by graphitic layers. Carbon 46:1417–1423

[51] Zhu J, Luo Z, Wu S, Haldolaarachchige N, Young DP, Wei S, Guo Z (2012) Magnetic graphene nanocomposites: electron conduction, giant magnetoresistance and tunable negative permittivity. J Mater Chem 22:835–844

[52] Brack N, Kappen P, Spencer MJS, Herries AIR, Rider AN (2016) Manipulation of carbon nanotube magnetism with metal-rich iron nanoparticles. J Mater Chem C 4:1215–1227

[53] Lassegue P, Noe L, Monthioux M, Caussat B (2015) Iron deposition on multi-walled carbon nanotubes by fluidized bed MOCVD for aeronautic applications. Phys Status Solidi C 12:861–868

[54] Brack N, Kappen P, Herries AIR, Trueman A, Rider AN (2014) Evolution of magnetic and structural properties during iron plating of carbon nanotubes. J Phys Chem C 118:13218–13227

[55] Manasrah AD, Al-Mubaiyedh UA, Laui T, Ben-Mansour R, Al-Marri MJ, Almanassra IW, Abdala A, Atieh MA (2016) Heat transfer enhancement of nanofluids using iron nanoparticles decorated carbon nanotubes. Appl Therm Eng 107:1008–1018

[56] Masipa PM, Magadzu T, Mkhondo B (2013) Decoration of multi-walled carbon nanotubes by metal nanoparticles and metal oxides using chemical evaporation method. S Afr J Chem 66:173–178

[57] Shanbedi M, Heris SZ, Amiri A, Eshghi H (2016) Synthesis of water-soluble Fe-decorated multi-walled carbon nanotubes: a study on thermo-physical properties of ferromagnetic nanofluid. J Taiwan Inst Chem Eng 60:547–554

[58] Detriche S, Devillers S, Seffer J-F, Nagy JB, Mekhalif Z, Delhalle J (2011) The use of water-soluble pyrene derivatives to probe the surface of carbon nanotubes. Carbon 49:2935–2943

[59] Martis P, Venugopal BR, Seffer J-F, Delhalle J, Mekhalif Z (2011) Infrared irradiation controlled decoration of multiwalled carbon nanotubes with copper/copper oxide nanocrystals. Acta Mater 59:5040–5047

[60] Venugopal BR, Detriche S, Delhalle J, Mekhalif Z (2012) Effect of infrared irradiation on immobilization of ZnO nanocrystals on multiwalled carbon nanotubes. J Nanopart Res 14:1079

[61] Maho A, Detriche S, Delhalle J, Mekhalif Z (2013) Sol–gel synthesis of tantalum oxide and phosphonic acid-modified carbon nanotubes composite coatings on titanium surfaces. Mater Sci Eng C 33:2686–2697

[62] Maho A, Detriche S, Fonder G, Delhalle J, Mekhalif Z (2014) Electrochemical co-deposition of phosphonate-modified carbon nanotubes and tantalum on nitinol. ChemElectroChem 1:896–902

[63] Lhost O, Bouvy C, Detriche S, Delhalle J, Mekhalif Z, Vachaudez M, Devahif T (2014) Process for covalently grafting a carbonaceous material. WO2014/184330 A1

[64] Chungchamroenkit P, Chavadej S, Yanatatsaneejit U, Kitiyanan B (2008) Residue catalyst support removal and purification of carbon nanotubes by NaOH leaching and froth flotation. Sep Purif Technol 60:206–214

[65] Okpalugo TIT, Papakonstantinou P, Murphy H, McLaughlin J, Brown NMD (2005) High resolution XPS characterization of chemical functionalised MWCNTs and SWCNTs. Carbon 43:153–161

[66] Datsyuk V, Kalyva M, Papagelis K, Parthenios J, Tasis D, Siokou A, Kallitsis I, Galiotis C (2008) Chemical oxidation of multiwalled carbon nanotubes. Carbon 46:833–840

[67] Arrotin B, Delhalle J, Dubois P, Mespouille L, Mekhalif Z (2017) Electroassisted functionalization of nitinol surface, a powerful strategy for polymer coating through controlled radical surface initiation. Langmuir 33:2977–2985

[68] Hou P-X, Liu C, Cheng H-M (2008) Purification of carbon nanotubes. Carbon 46:2003–2025

[69] Dujardin E, Ebbesen TW, Krishnan A, Treacy MMJ (1998) Purification of single-shell nanotubes. Adv Mater 10:611–613

[70] Rinzler AG, Liu J, Dai H, Nikolaev P, Huffman CB, Rodríguez-Macías FJ, Boul PJ, Lu AH, Heymann D, Colbert DT, Lee RS, Fischer JE, Rao AM, Eklund PC, Smalley RE (1998) Large-scale purification of single-wall carbon nanotubes: process, product, and characterization. Appl Phys A 67:29–37

[71] Hu H, Zhao B, Itkis ME, Haddon RC (2003) Nitric acid purification of single-walled carbon nanotubes. J Phys Chem B 107:13838–13842

[72] Zhao X, Ohkohchi M, Inoue S, Suzuki T, Kadoya T, Ando Y (2006) Large-scale purification of single-wall carbon nanotubes prepared by electric arc discharge. Diamond Relat Mater 15:1098–1102

[73] Suzuki T, Suhama K, Zhao X, Inoue S, Nishikawa N, Ando Y (2007) Purification of single-wall carbon nanotubes produced by arc plasma jet method. Diamond Relat Mater 16:1116–1120

[74] Wang Y, Shan H, Hauge RH, Pasquali M, Smalley RE (2007) A highly selective, one-pot purification method for singlewalled carbon nanotubes. J. Phys. Chem. B 111:1249–1252

[75] Zhang J, Zou H, Qing Q, Yang Y, Li Q, Liu Z, Guo X, Du Z (2003) Effect of chemical oxidation on the structure of single-walled carbon nanotubes. J Phys Chem B 107:3712–3718

[76] Colomer J-F, Piedigrosso P, Fonseca A, Nagy JB (1999) Different purification methods of carbon nanotubes produced by catalytic synthesis. Synth Met 103:2482–2483

[77] Hernadi K, Siska A, Thien-Nga L, Forro L, Kiricsi I (2001) Reactivity of different kinds of carbon during oxidative purification of catalytically prepared carbon nanotubes. Solid State Ion 141–142:203–209

[78] Su S-H, Chiang W-T, Lin C-C, Yokoyama M (2008) Multi-wall carbon nanotubes: purification, morphology and field emission performance. Phys E 40:2322–2326

[79] Sadegh H, Shahryari-ghoshekandi R, Kazemi M (2014) Study in synthesis and characterization of carbon nanotubes decorated by magnetic iron oxide nanoparticles. Int Nano Lett 4:129–135

[80] Zhang Q, Zhu M, Zhang Q, Li Y, Wang H (2009) The formation of magnetite nanoparticles on the sidewalls of multi-walled carbon nanotubes. Compos Sci Technol 69:633–638

[81] Cun-ku D, Xin L, Yan Z, Jing-yao Q, Yun-fang Y (2009) $Fe_3O_4$ nanoparticles decorated multi-walled carbon nanotubes and their sorption properties. Chem Res Chin Univ 25:936–940

[82] Shanbedi M, Heris SZ, Amiri A, Eshghi H (2016) Synthesis of water-soluble Fe-decorated multi-walled carbon nanotubes: a study on thermo-physical properties of ferromagnetic nanofluid. J Taiwan Inst Chem Eng 60:547–554

[83] Masoomi-Godarzi S, Khodadadi AA, Vesali-Naseh M, Mortazavi Y (2014) Highly stable and selective non-enzymatic glucose biosensor using carbon nanotubes decorated by $Fe_3O_4$ nanoparticles. J Electrochem Soc 161:B19–B25

[84] Lv X, Xu J, Jiang G, Xu X (2011) Removal of chromium(VI) from wastewater by nanoscale zero-valent iron particles supported on multiwalled carbon nanotubes. Chemosphere 85:1204–1209

[85] Jiao W, Feng Z, Liu Y, Jiang H (2016) Degradation of nitrobenzene-containing wastewater by carbon nanotubes immobilized nanoscale zerovalent iron. J Nanopart Res 18(198):1–9

[86] Singhal RK, Gangadhar B, Basu H, Manisha V, Naidu GRK, Reddy AVR (2012) Remediation of malathion contaminated soil using zero valent iron nano-particles. Am J Anal Chem 3:76–82

[87] Sun Y-P, Li X-Q, Cao J, Zhang W-X, Wang HP (2006) Characterization of zero-valent iron nanoparticles. Adv Colloid Interface Sci 120:47–56